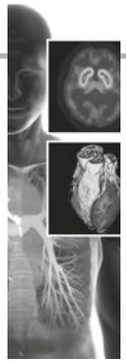

Imaging innovations for cancer therapy response monitoring

Innovative imaging approaches for monitoring various types of cancer treatment response are discussed in this paper. Radionuclide imaging has demonstrated favorable capabilities for imaging tumor response based on the binding of radionuclides to the cells responding to the treatment. MRI has recently been utilized for detecting the cellular changes associated with apoptosis. Dynamic contrast-enhanced ultrasound has been proposed for monitoring therapeutics that target blood vessels affecting perfusion. Quantitative ultrasound has been demonstrated to be capable of differentiating between viable cell clusters and clusters responding to treatment. Diffuse optical imaging and photoacoustic imaging have been applied for evaluating functional changes transpiring in soft tissue, such as oxygenation status, during cancer treatment. Considerable developments introduced to improve the precision of treatment response monitoring are expected in the near future to provide clinical approaches to personalized therapy in which therapies can be adapted based on the detection of functional physiology-based responses.

KEYWORDS: cancer ▪ cell death ▪ DCE-US ▪ DOI ▪ functional imaging ▪ MRI ▪ perfusion ▪ PET ▪ QUS ▪ SPECT ▪ therapy response

Ali Sadeghi-Naini[1,2,3,4], Omar Falou[1,2,3,4], John M Hudson[1,3], Colleen Bailey[1,3], Peter N Burns[1,3], Martin J Yaffe[1,3], Greg J Stanisz[1,3], Michael C Kolios [3,5] & Gregory J Czarnota*[1,2,3,4]

[1]Department of Imaging Research, Sunnybrook Health Sciences Centre, Toronto, ON, Canada
[2]Department of Radiation Oncology, Sunnybrook Health Sciences Centre, Toronto, ON, Canada
[3]Department of Medical Biophysics, University of Toronto, Toronto, ON, Canada
[4]Department of Radiation Oncology, University of Toronto, Toronto, ON, Canada
[5]Department of Physics, Ryerson University, Toronto, ON, Canada
**Author for correspondence:*
Tel.: +1 416 480 6100 ext. 7073
Fax: +1 416 480 6002
gregory.czarnota@sunnybrook.ca

Cancer therapy response monitoring

Personalized medicine is predicated on changing an ineffective therapy to one that is more efficacious for a specific patient. Therapy response monitoring using imaging methods is an important component of personalized medicine. In cancer treatment, standard anatomical-based imaging can detect macroscopic changes in tumor size, but these often take many weeks to months to develop. Functional imaging methods that probe tumor physiology have recently been demonstrated capable of detecting tumor responses from days to weeks after starting therapy. Such methods could be used to guide, noninvasively, changes in treatment in order to optimize the chances of cure. They could be utilized to change ineffective therapies after only days of use, instead of waiting many months to find no effect.

A number of imaging-based methods have recently been developed that can detect cell death in tumor responses to treatment as reviewed in [1]. These include 2-[^{18}F]-fluoro-2-deoxy-D-glucose PET (FDG-PET) and [1-^{13}C]-hyperpolarized pyruvate imaging as markers of tumor glucose metabolism, 3′-deoxy-3′-^{18}F-flurothymidine (FLT) for DNA synthesis, and PET and magnetic resonance spectroscopy (MRS) for amino acid and lipid metabolism. In addition, specialized methods in MRI and quantitative ultrasound (QUS) have recently been developed to detect cell death, which can also be used to track the effects of therapy [2,3]. Other methods for cell death detection include antibody-based labeling imaging using SPECT, PET, MRI and optical imaging, all of which can potentially be used to guide personalized therapy.

Using breast cancer as an example, patients with locally advanced breast cancer (LABC) represent a typical patient population who benefit from changing ineffective therapies to more efficacious treatments. Breast cancer is the most common malignancy for females in North America. Approximately 5–15% of the estimated 200,000 new cases diagnosed each year will present with LABC [4–5]. LABC has variable definitions, including stage III disease or inoperable disease. For the purposes of this review, the data presented are restricted to women with tumors greater than 5 cm and/or tumors with chest wall or skin involvement (i.e., T3 or T4 disease in the breast), with or without clinical nodal involvement, but with no evidence of distant metastatic disease. LABC carries a much poorer prognosis compared with early stages, with only 55% of LABC patients surviving at 5 years because of the high risk for metastatic spread [6]. Also, despite aggressive therapeutic combinations, including chemotherapy, surgery and radiation therapy (RT), the locoregional recurrence rate remains high at 10–20% [6].

The current treatment of LABC includes aggressive neoadjuvant chemotherapy followed

Future Medicine part of fsg

by surgery that is generally a mastectomy with axillary nodal clearance, followed by radiation treatment and possibly herceptin and/or hormonal manipulation, if indicated [7–9]. Several authors have pointed out the importance of clinical and pathological complete response to neoadjuvant chemotherapy as a marker of better outcomes, with survival rates reaching 70% [10,11]. This better prognosis could be related to the selection of patients with more chemotherapy-sensitive tumors, or may be related to improved loco-regional control. Along this line, a recent update of the Early Breast Cancer Trialists Collaborative Group (EBCTCG) meta-analysis demonstrated a significant improvement in overall survival for node-positive patients who received adjuvant radiation treatment, compared with those treated with surgery alone [12,13]. These findings stress the importance of locoregional control as a way to improve the outcomes for LABC. Several trials are aiming at optimizing the chemotherapy combination to evaluate the benefit of concomitant radiation and chemotherapy to maximize the rate of pathological complete response.

However, the search for the optimal LABC treatment remains controversial because determining the optimal treatment paradigm is fraught with uncertainties, both in terms of treatment regimen and duration of treatment [8,9]. While complete pathological response to neoadjuvant chemotherapy has been shown to correlate strongly with patient survival [14] this prognostic factor is assessed at the time of surgery, as after this point the window for a neoadjuvant treatment is closed. Conventional clinical surrogates based on anatomical information from ongoing physical assessment, and standard clinical imaging methods such as mammography and B-mode ultrasound (US) suffers from an inability to objectively assess treatment response early during the course of treatment [15]. Subjective physical assessment is also not quite reliable, especially at early treatment stages, as analyzed from our own institutional patient data. Out of 250 patients with LABC treated over the last 4 years, data indicate that only one out of 250 patients were switched to salvage therapy on the basis of clinical examination after one cycle of chemotherapy. Most of the women whose disease was ultimately refractory to chemotherapy (n = 50) were offered salvage therapy only after 4–5 cycles of chemotherapy (3–4 months after initiating chemotherapy) when physical examination was used as a response detector.

The early detection of patients refractory to chemotherapy is critical, and indication of this can be seen in a study by Huang *et al.*, who have shown that salvage treatment for chemotherapy-resistant (nonresponsive) tumors with LABC can result in a survival rate of 46% at 5 years [16]. Surgery alone at this stage is often not possible. Thus, the detection of nonresponsive tumors could facilitate the switch to early salvage therapy. Consequently, imaging for early detection of response or absence of response is very important [17]. Objective, low-cost functional imaging methods capable of assessing tumor response to guide the tailoring of therapy could thus be very useful.

Potential methods, including radionuclide imaging, MRI techniques, dynamic contrast-enhanced US (DCE-US), QUS methods for cell death detection, diffuse optical imaging (DOI) methods and photoacoustic imaging (PAI), are discussed later as emerging methods to carry out such functional analyses. Such methods could soon enhance the development of personalized medicine.

Radionuclide imaging: visualizing cellular biology, metabolism & receptor expression

Radionuclide imaging, including PET and SPECT, can be used for evaluating measures that reflect cellular biochemistry, biology, metabolism and receptor expression [1]. Such functional measures can provide an earlier classification of treatment responders or nonresponders, in comparison to using standard tumor size measures, which can occur later during treatment.

PET has been applied to the monitoring of cellular glucose consumption via visualizing glucose analog uptake using FDG [18], which has been shown to correlate with a number of viable cancer cells [19]. FDG-PET has exhibited a specificity and sensitivity of near 90% for identifying primary and metastatic tumors in various cancer patients [20]. It has also been demonstrated to have capabilities for distinguishing responding patients early following therapy [21–23]. PET has also been employed to evaluate tumor cell proliferation through visualizing 2[^{11}C]thymidine and FLT uptake [24,25]. This has been found to demonstrate capabilities of early therapy response prediction in breast cancer patients [26]. PET has also been shown to be capable of imaging hypoxia, which is observed in 50–60% of all solid tumors [27]. Imaging of hypoxia using PET has demonstrated potential for the monitoring of response or even predicting upfront therapy

response [28,29]. SPECT, an earlier technology, and PET can both be utilized for detecting programmed cell death by tracing phosphatidylserine, which is exposed on the outer leaflet of the plasma membrane bilayer in early stages of apoptosis [30,31]. This marker has, however, not been found to be very specific for apoptotic cell death with cross-reactivity to cells in other states of cell death.

These techniques have been also used for imaging receptors on the tumor cell surface [32]. Androgen and estrogen receptor expression have been evaluated in prostate and breast cancer tumors by imaging [^{18}F]fluoro-oestradiol and 16-[^{18}F]fluoro-5-dihydrotestosterone uptakes, respectively, where both were found to have correlations with treatment response [33,34]. Radionuclide imaging techniques have recently been adjusted for visualizing tumor-associated overexpression of antigens, such as HER2, using affibody molecules [35,36]. Affibody molecules are a newly introduced class of tiny 7-kDa phage display-selected affinity proteins. Their major advantage over antibodies is due to their much smaller size, and they are capable of more rapid tumor localization in addition to a more rapid clearance from nonspecific compartments. Pilot clinical studies using indium-111 and gallium-68-labeled anti-HER2 affibody tracer have demonstrated their ability for monitoring tumor response in cancer patients [37]. PET, however, requires radionuclides and remains limited in resolution due to limitations in positron detection. Moreover, the injection of radionuclides limits number of times patients would be imaged during their therapy to assess tumor response. Other methods, including MRI, offer potential for nonradiolabeled imaging at higher spatial resolutions.

MRI: measuring water relaxation, diffusion & exchange

Conventional MRI techniques such as T_1 and T_2 relaxation and diffusion of water are sensitive to the environment around the water molecules being measured. They therefore provide possibilities for monitoring therapy response via the breakdown of macromolecules, loss of membrane integrity, change in cell size and change in water content occurring during cell death. However, these changes have typically been detected only at late stages of apoptosis, when there is a decrease in cell density and an increase in extracellular water [38,39]. Figure 1A & B shows the late change in conventional T_1 and T_2 relaxation times in an *in vitro* model where apoptosis was induced in acute myeloid leukemia (AML) cells using cisplatin, and cells imaged 36 and 48 h after treatment. The apoptotic cell death fractions induced by cancer therapy at these times are presented in Figure 1F for comparison. Recent work offers some explanation of the low sensitivity of these techniques to cell death and suggests ways to improve it, as follows.

Conventional T_1 relaxation time measurements at common clinical frequencies of 1–3 T depend on motions mainly from free water protons. One method of probing the motion of protons on larger macromolecules uses complex imaging methods which rely on T_1 relaxation in the rotating frame, $T_{1\rho}$. With this technique, contributing molecular motion frequencies are determined by the strength of a spin-locking pulse, where appropriate strength yields $T_{1\rho}$, which increases at earlier stages of apoptosis than conventional relaxation [40–42]. However, $T_{1\rho}$ studies [40] and the closely related technique of magnetization transfer [43] have shown that these changes are related mainly to an increase in extracellular water. Figure 1C shows the magnetization transfer ratio (MTR) after apoptosis is induced; however, this change is not significant even at late stages of apoptotic cell death.

It is also possible for pH changes during apoptosis to affect $T_{1\rho}$, but other methods such as chemical exchange saturation transfer (CEST) are more commonly used to examine pH. CEST has been related to cellularity in brain tumor xenografts [44] and so offers additional promise for therapy monitoring. $T_{1\rho}$, magnetization transfer and CEST all involve the use of long radiofrequency pulses, which are limited by the amount of energy that can be deposited into the body (i.e., the specific absorption rate). In addition, these methods can be technically difficult to implement, both because the concentrations of macromolecules that need to be detected are low and because good B_0 and B_1 field homogeneity are needed (i.e., this is a low signal-to-noise ratio estimate).

Conventional relaxation measurements can also be affected by the rate of water exchange between intracellular and extracellular environments. This exchange is much faster than typical T_1 relaxation times, but relaxation can be altered by the addition of extracellular contrast agents, such as the clinically used Gd-DTPA and its low molecular weight derivatives. With a wide enough range of contrast agent concentrations, the exchange rate of water across the cell membrane, along with the extracellular water fraction (Figure 1D & E), can be determined and this has

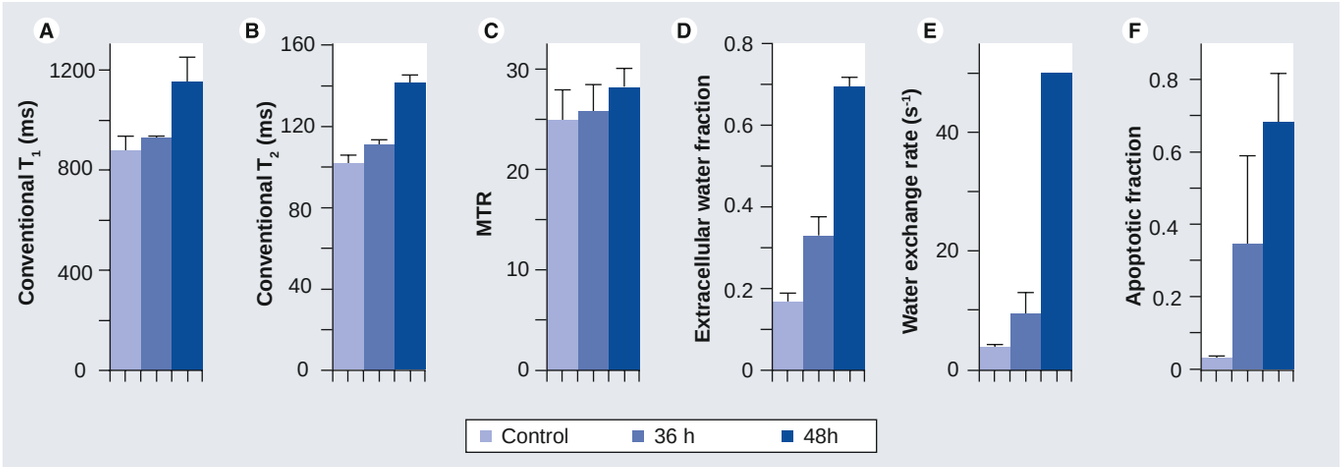

Figure 1. MRI parameters of cell death. Data presented is from studies of acute myeloid leukemia cell samples at 1.5 T **(A–E)** compared with the fraction of cells undergoing apoptosis **(F)** 36 and 48 h after treatment with the chemotherapy drug cisplatin. Apoptotic counts were based on cells exhibiting nuclear condensation on H&E staining (confirmed by TUNEL). **(A)** Conventional T_1 and **(B)** T_2 relaxation times show relatively small changes at late stages of treatment. **(C)** The change in magnetization transfer ratio is not statistically significant. **(D)** The extracellular water fraction and **(E)** water exchange rate from relaxation studies in the presence of the contrast agent Gd-DTPA-BMA show changes at the earlier 36-h time-point.
MTR: Magnetization transfer ratio.

shown promise *in vitro* as a marker of apoptosis [45] owing to the relation of exchange to cell size, shape and particularly membrane integrity.

In vivo, gadolinium-based contrast agents have mainly been employed in dynamic contrast-enhanced MRI (DCE-MRI), as recently reviewed in [46,47], but often with a focus on vascular changes and the assumption of fast water exchange. Exchange itself has frequently been viewed as a hindrance because it can produce incorrect values for the volume transfer constant, K_{trans}, and the extravascular extracellular water fraction, v_e. Therefore, the research focus has often been on minimizing the effect of exchange on these parameters by limiting the amount of contrast agent injected or through the appropriate selection of scan parameters [48]. Nevertheless, given the usefulness of exchange as a marker of nonvascular, apoptotic change, contrast-enhanced methods that are more sensitive to exchange are being developed.

Clinical work using three different flip angles at the late stages of contrast agent uptake has permitted estimation of exchange [49], although the amount of data collected limits precision. To be sensitive, measurements need to be made at multiple flip angles for a range of contrast agent concentrations. Longer repetition times (TRs) with well-chosen flip angles will give higher signals and greater sensitivity to exchange. However, longer repetition times and more flip angles decrease temporal resolution, which is particularly important to obtain accurate pharmacokinetic parameters. Alternate injection methods may lessen temporal resolution restrictions. Detailed T_1 measurements during a steady-state infusion have been done in the past [50], but require long waiting periods to reach steady-state. Recent work indicates that slower injection of the contrast agent bolus [51] or multiple injections [2,52] may loosen temporal resolution requirements and allow for the more detailed T_1 measurements in the tissue that are needed to determine exchange precisely. Preliminary work during only the slowly varying late portion of uptake following three separate Gd-DTPA-BMA injections in a rat xenograft model showed that, with four flip angles at each contrast agent concentration, parametric maps of the extracellular water fraction (Figure 2A) and the water exchange rate across the plasma membrane (Figure 2B) could be obtained. This method is not valid in all regions; areas of low uptake or areas where uptake is not at steady-state have been eliminated from the maps. Nevertheless, the parameters show correlation when compared with histology (Figure 2C & D).

Conventional diffusion measurements of therapy response are related mainly to tumor cellularity. Separation of intracellular and extracellular diffusion and determination of water exchange are theoretically possible without contrast agents, using a standard diffusion sequence, but only at high gradient strengths [53]. Information at smaller length scales is limited by the range of diffusion times available. Short diffusion times invalidate the assumption that motion during the gradients is negligible

relative to motion during the diffusion time. There are, however, methods of altering the diffusion sequence to obtain shorter diffusion times. A conventional diffusion sequence has two gradient lobes with constant amplitude separated by a diffusion time, but it is possible to vary the gradient amplitude over time, sinusoidally for example. This yields a sequence sensitive to diffusion with particular frequency components. High frequencies correspond to short diffusion times, and thus restrictions can be seen not just on the cellular level, but on much shorter distance scales. Such oscillating gradient sequences have been shown to be sensitive to intracellular changes such as cytoskeleton disruption [54] and nuclear size [55]. This technique has been applied to a rat brain tumor model and found greater contrast and heterogeneity following treatment than in images obtained with conventional diffusion measurements [56]. This technique is improved by higher gradient strengths and these are becoming more common clinically. Therefore, this method offers promise in monitoring cell death for therapy response.

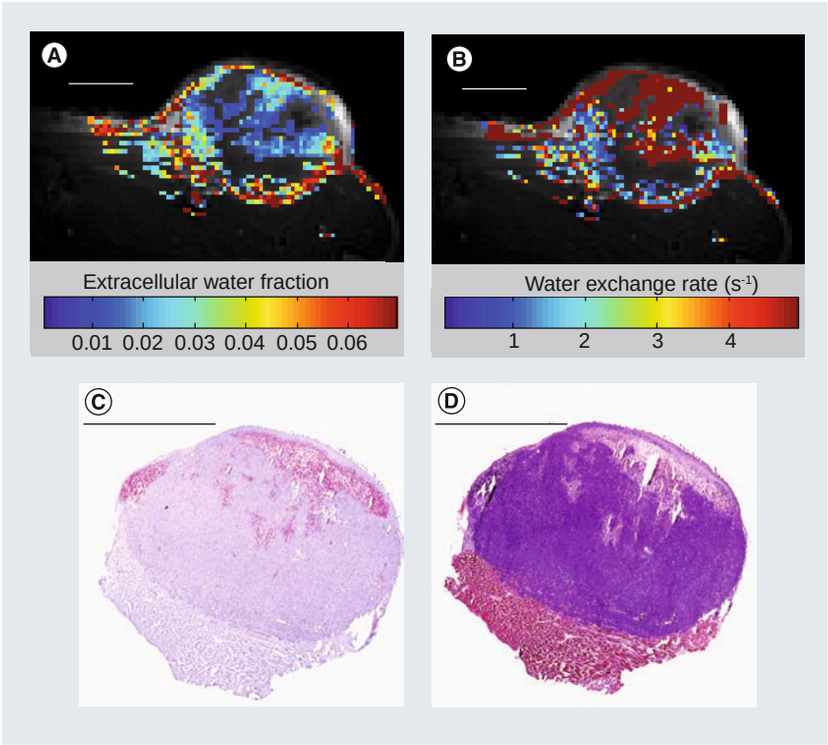

Figure 2. Parametric maps from T_1 relaxation measurements of cell death. Maps were made from data acquired during the slowly varying late-uptake stage following contrast agent injection in a xenograft model in the hind limb of a rat. **(A)** The fraction of water that is extracellular and **(B)** the exchange rate of water from the intracellular to extracellular spaces. Many areas with higher extracellular water fraction correlate to lighter areas on **(C)** H&E-stained slides. **(D)** Areas that stain positively on TUNEL correlate to areas with high water exchange. Scale bar represents 10 mm in **(A & B)** and 5 mm in **(C & D)**.

DCE-US: imaging blood perfusion

Blood perfusion is a physiological parameter of significant experimental and clinical importance that reflects the adaptive response of organs to their normal biological environment, to disease, trauma and the malignant progression of cancer [57]. Perfusion is also intrinsically linked to the efficacy of therapeutic interventions, including radiotherapy [58], thermal [59] and drug therapy [60], where treatment success relies on adequate tissue oxygenation, temperature distributions and sufficient vascular access of drugs to their molecular targets, respectively.

Currently, a variety of medical technologies, such as contrast CT, contrast MR and PET, are clinically available to generate perfusion maps. These techniques rely upon the external detection of exogenous tracers that can be distinguished from tissue and whose dynamics are related to physiological features (blood flow, vascular volume, vascular morphology and permeability, among others) of the microvasculature. DCE-US is a promising modality that combines the strengths of diagnostic US imaging (i.e., fast, portable, safe, widely available and cost effective) with the unique properties of intravascular microbubble contrast agents to visualize and quantify the blood volume and flow velocities in organs and solid tumors. Recently, DCE-US perfusion measurements have been demonstrated to correlate with coregistered DCE-MRI and other gold standard measures of organ blood flow [61,62].

US contrast agents comprise nontoxic micron-sized bubbles (1–10 µm diameter) of high molecular weight gas encapsulated by a thin, biocompatible shell [63,64]. As a tracer, microbubbles are confined to the blood pool and travel with similar kinetics to red blood cells [65]; microbubbles are easily discriminated from surrounding tissues due to the large acoustic impedance mismatch with the blood, as well as their acoustic resonance at the diagnostic frequency range [66]; and the relationship between the microbubble concentration and the attenuation-corrected backscattered echo used for quantification is linear (up to a certain concentration) [67].

Therapy response monitoring using DCE-US is performed by measuring the time–intensity course of an intravenous bolus of microbubble contrast agent as it passes through the imaging plane [68,69]. Characteristics of the microvasculature and microcirculation can be extracted directly from the shape of the time–intensity curve (e.g., area under the curve, time to peak

intensity and mean transit time, among others), providing an easy (model free), reasonably reproducible semi-quantitative measurement [69,70]. Alternatively, quantification of blood flow can also be accomplished by recording the replenishment of the imaging plane following the local disruption of the contrast agent during a constant infusion, using a method first proposed for myocardial perfusion [71]. Recent models of microbubble replenishment kinetics have further improved the reproducibility of clinical perfusion measurements [72,73]. Quantifying the time–intensity curve of a constant infusion and disruption–replenishment measurement is simpler in practice because with bolus measurements, effectively close to a delta function, increased contrast is generated directly within the site of measurement, whereas using constant infusion methods avoids the unknown influence of cardiopulmonary transit. In addition, constant infusion methods offer the practical advantage that many measurements can be made in multiple anatomic planes during a single infusion, allowing a quasi 3D assessment of tumor microvascularity.

DCE-US is currently used to monitor a variety of clinical interventions, including guiding and evaluating radiofrequency ablation (RFA) therapy [74–76], assessing therapeutic response to radiotherapy [77], and monitoring inflammatory activity during the relapse and remittance of Crohn's disease [78]. One of the most promising applications of DCE-US is to monitor changes in vascularity and perfusion within tumors being treated with vascular disrupting and anti-angiogenic agents (**Figure 3**) [68,79,80]. In a recently published study [68], DCE-US identified patients that were responding to anti-angiogenic drugs for metastatic renal cell carcinoma within 2 weeks after the start of treatment. In the near future, DCE-US may be used to efficiently identify promising antivascular agents in the preclinic, promptly identify responding patients and assist with the individualization of patient care.

QUS: monitoring cell death response

Cell death introduces structural changes in the cell's nucleus including nuclear condensation and fragmentation. We have previously demonstrated that nuclear structure is closely linked to US backscatter properties of cells and tissues for high-frequency US. The changes in nuclear structure associated with cell death, hence results in differentiable echogenicities of living cells, necrotic cells and cells dying of programmed cell death or apoptosis. This has been confirmed through several studies conducted *in vitro*, *in situ*, *ex vivo* and *in vivo* [3,81–88,89]. US radiofrequency (RF) signals carry information about tissue echogenicity but until recently have not been readily accessible on commercial US systems. Since a large number of instrument parameters are involved in a typical US imaging and data acquisition session, it is difficult to establish a reasonable comparison between imaging data acquired by different standard US machines, or even by the same machine when different settings are used. QUS methods have been proposed to address this shortcoming. QUS analyzes the acquired raw data before it is envelope detected, log amplified and processed to form a B-mode US image and employs calibration techniques to provide parameter estimates, which are predominantly independent of instrument settings. Such estimates are frequently based on backscatter analysis of RF echoes and include the integrated backscatter, RF envelope statistics, frequency dependence of the backscatter, US tissue attenuation, and, in a broader sense, can include elastic properties of tissues, propagation of shear waves in tissues, and other signal classification techniques such as entropy metrics of RF ultrasonic backscatter [90,91]. Different subsets of these parameters have been utilized in a number of clinically related applications and particularly for tissue classification purposes such as differentiating benign versus malignant disease [92–99].

The application of QUS techniques for the detection of cell death is a relatively new development [100,101]. High-frequency (20–60 MHz) QUS parameters have been found in preclinical animal tumor experiments to demonstrate reproducible and statistically significant features in the US signals that are associated with cell death. The methods are robust and can be applied to detecting and determining the extent of cell death from different anticancer therapies [3,84,89]. This is because high-frequency US is particularly sensitive to the structural changes that cells and tissues undergo during treatment response [82,86,88]. Such changes, including nuclear condensation and fragmentation, frequently result in substantial increases in tissue echogeneity and consequently cause a large boost in backscatter signal. Other factors such as cell shape may also contribute, but the nuclear changes associated with cell death have been demonstrated to be responsible for the contrast in QUS parameters. In this context, whereas high-frequency US provides better lateral and axial resolutions (tens

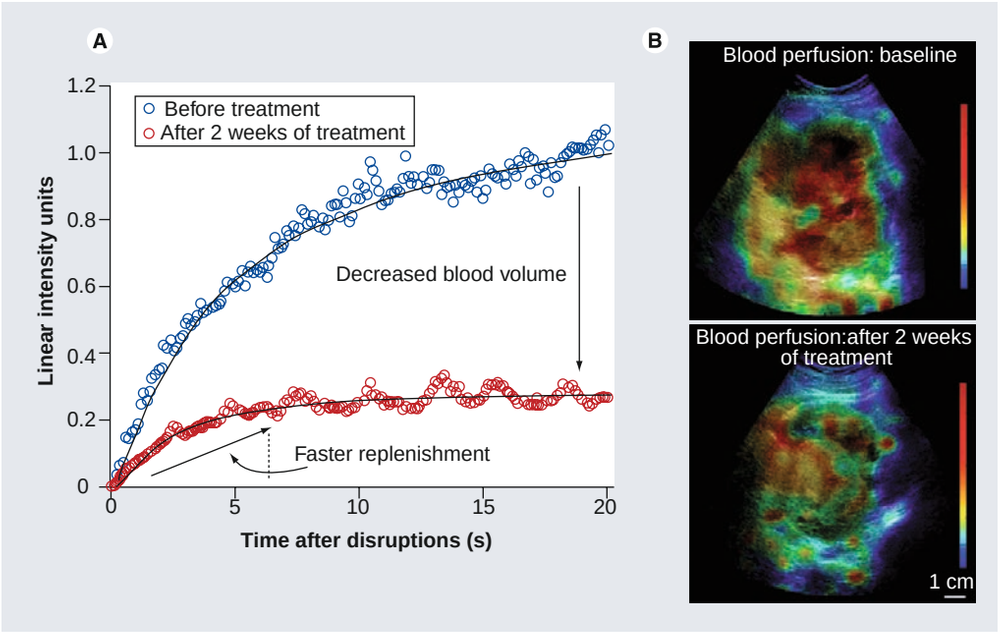

Figure 3. Tumor response to anti-angiogenic therapy can be monitored with dynamic contrast-enhanced ultrasound. (A) Parameters that quantify tumor blood volume, flow velocity and perfusion are extracted from the kinetics of microbubble replenishment. Dynamic contrast-enhanced ultrasound methods are able to quantify changes in the tumor vasculature in as little as 1–2 weeks of treatment. Shown here, anti-angiogenic drugs reduce the blood volume of this renal cell carcinoma by approximately 80%. An increase in the replenishment speed suggests that the therapy is targeting the smaller vessels and capillaries. **(B)** Replenishment kinetics can be quantified on a pixel-by-pixel basis to supplement anatomical images with functional overlays. The spatial distribution of vascular parameters can provide additional indices (i.e., heterogeneity) of tumor response.

of microns), its clinical application is limited due to a limited depth of US penetration [102]. Conventional (low-) to mid-range US frequencies (1–20 MHz) have much deeper penetration and are hence broadly used in medicine, and very recently have been used to monitor cell death response to cancer treatment with QUS methods, as described later.

Whereas the detection of tissue changes related to necrosis using US methods were measured nearly 50 years ago, it is only very recently that quantitative methods have been applied using clinical US frequencies. In a set of recent studies, conventional US (3–10 MHz, 6 dB bandwidth) was used for real-time detection of cell death using well-controlled AML cell culture experiments. Results demonstrated an ability to detect as little as 10% apoptotic cells using US frequencies in the 10 MHz range, paralleling changes observed using high-frequency US [3,101,103]. Time-course experiments indicate that changes are detectable as early as 6 h after exposure to chemotherapy drugs. These findings have been confirmed *in vivo* using prostate cancer PC3 tumor xenografts in mice [101,104,105]. Here, large macroscopic areas of cell death were induced by novel anti-angiogenic agents in combination with radiation. Results based on experiments using over 50 animals assessed with high-frequency and conventional-frequency US suggests that the monitoring of treatment efficacy is possible at low-frequency US.

In a very recent pilot clinical study, QUS at conventional frequencies has been applied for evaluation of tumor cell death response in LABC patients receiving neoadjuvant chemotherapy [106]. Conventional US data were acquired prior to treatment onset and at four-times during treatment. In each session, several scan planes with the size of 6 × 4 cm were acquired from the same nominal regions. The RF signal's power spectrums were normalized at each region of interest using a reference's power spectrum obtained from an agar-embedded glass-bead phantom model, at the same region of interest's position. The results (n = 10 patients) demonstrated a close association between QUS changes after one to two cycles of chemotherapy (few weeks) and clinical response in the tumor many months later. More specifically, patients who had a significant clinical response demonstrated changes in QUS parameters consistent with cell death, while women with no changes in QUS parameters demonstrated no ultimate

clinical response (Figure 4). The promising results emerging from this study pave the way for establishing protocols for the clinical applications of the conventional frequency QUS techniques in therapy response monitoring. As such, QUS at conventional frequencies is expected to provide rapid and quantitative functional information in real time for evaluating responses to a specific therapy in the near future.

DOI: evaluating tissue functional & structural changes

The need for a noninvasive, nonionizing and inexpensive imaging modality to monitor treatment response has recently led to renewed interest in the potential of optical imaging. Conventional optical imaging methods were introduced in the 1920s in order to detect lesions in the breast [107]. However, these methods were not successful due to image distortions as a result of multiple light scattering. Recent advances in optical technologies in the past decade have led to an increased focus on the use of optical imaging modalities to diagnose and monitor treatment response [108].

DOI is a tomographic technique that employs near-infrared light to provide quantitative spectral information regarding the absorption and scattering properties of tissue [108,109]. There are three types of DOI systems: continuous wave, frequency domain and time domain. In continuous wave systems, light is emitted at constant amplitude and the intensity of light transmitted across the breast is measured. In frequency domain systems, the light is emitted continuously but its amplitude is modulated at a particular frequency. The intensity decay and phase shift of the emitted light are used to obtain optical properties of the tissue. In time domain systems, the tissue is illuminated with picosecond pulses of light. The temporal distribution of photons as they exit the tissue are measured and used to calculate tissue optical properties [110]. These can then be converted to parameters related to tissue microstructure and biochemical composition such as water, lipid and hemoglobin. Since optical contrast comes from intrinsic tissue components, DOI does not require exogenous markers making it ideal for treatment monitoring.

DOI has been shown to be capable of providing functional information related to brain activity [111–117]. In studies of breast tissue, DOI has been used to investigate the underlying physiological differences as a result of age, BMI, menopausal status and fluctuations in the menstrual cycle [118]. It has also been used to differentiate between normal and malignant breast tissue [119]. Angiogenesis, cellular proliferation, hypoxia and extracellular matrix breakdown are biological factors that have all been linked with cancer and were shown to directly influence the concentration of optical parameters such as total hemoglobin, water and lipid concentrations [119,120]. Clinical studies have indicated that DOI may provide useful information on whether or not a particular treatment regimen is successful [121–126].

In a recent study, DOI was used to monitor the response of breast cancer patients undergoing neoadjuvant chemotherapy [125]. Results have shown that optical parameters, such as oxyhemoglobin, deoxyhemoglobin, water and scattering power, can provide an indication of response within 4 weeks in patients undergoing various neoadjuvant treatments. Responders showed a significant reduction in these optical parameters within 4 weeks after starting the neoadjuvant treatment. By contrast, patients who did not respond well to the treatment showed little-to-no change in these parameters after treatment initiation as shown in Figure 5. A similar study showed that oxyhemoglobin increases significantly in responding patients, as opposed to nonresponding patients, which exhibited a decrease in oxyhemoglobin on day 1 after treatment initiation [122]. These studies demonstrate that there is a strong correlation between the treatment response and the changes in the functional and structural optical parameters.

PAI: contrasting changes in blood volume & oxygenation status

A hybrid imaging technology that involves optical illumination and US detection is PAI. Even though the photoacoustic effect has been known for over a hundred years (first discovered by Bell in 1880 [127]), it has only recently evolved as a biomedical imaging modality with commercial systems now available [201–203]. In typical PAI systems, short laser pulses (in the order of a few nanoseconds) are used to illuminate the target tissues. Tissue structures that absorb the optical energy heat up, rapidly expand and then gradually contract as energy is lost through thermal diffusion to the surrounding tissue. The rapid expansion creates a photoacoustic pressure wave that can then be detected with conventional US technology. The main tissue structure that absorbs the majority of the propagating light in the near-infrared spectral range is the red blood cell. The absorption coefficient ratio between blood and surrounding tissues is as high as

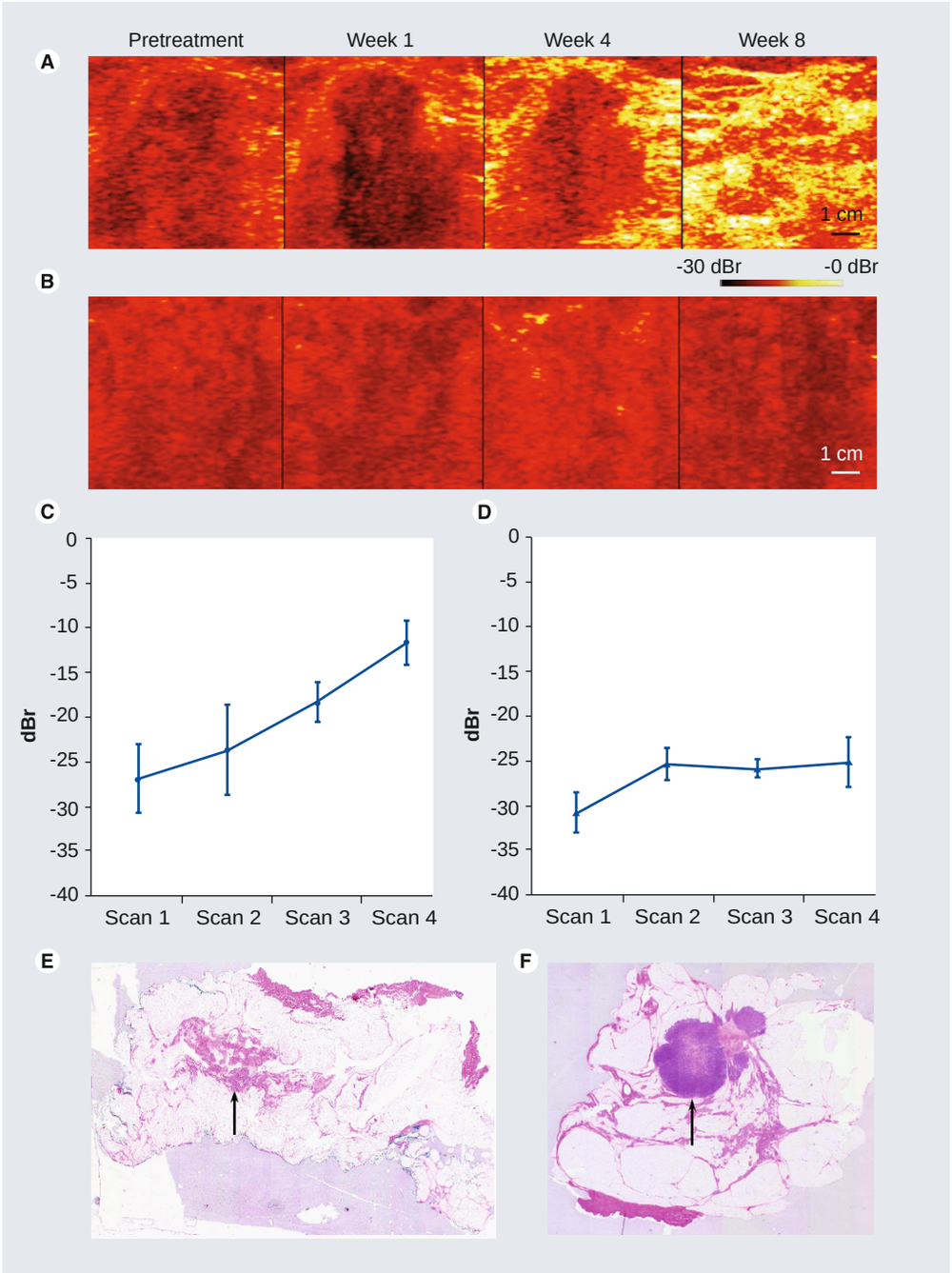

Figure 4. The application of conventional frequency quantitative ultrasound for monitoring tumor cell death response. (A & B) Representative parametric 0-MHz intercept images of a large tumor during neoadjuvant chemotherapy for a **(A)** clinically responding patient, **(B)** clinically nonresponding patient. **(C & D)** Quantitative 0-MHz intercept data averaged over the tumor area for the **(C)** clinically responding patient, **(D)** clinically nonresponding patient. Scans 1, 2, 3 and 4 correspond to the pretreatment scan, and the scans acquired at week 1, 4 and 8, respectively. At scan 3 (4 weeks) of the clinically responding patient an increase in intercept is apparent compared with scan 1 (pretreatment). In the case of the clinically nonresponding patient there is no striking change in the 0-Mhz intercept during the majority of therapy compared with the case of a clinically responding patient. **(E)** The whole mount pathology corresponding to the clinically responding patient indicates a small residual mass (identified by the arrow) in the mastectomy specimen (10-cm wide). **(F)** The whole mount pathology corresponding to the clinically nonresponding patient indicates a large compact residual mass (identified by the arrow) in the mastectomy specimen (8-cm wide).

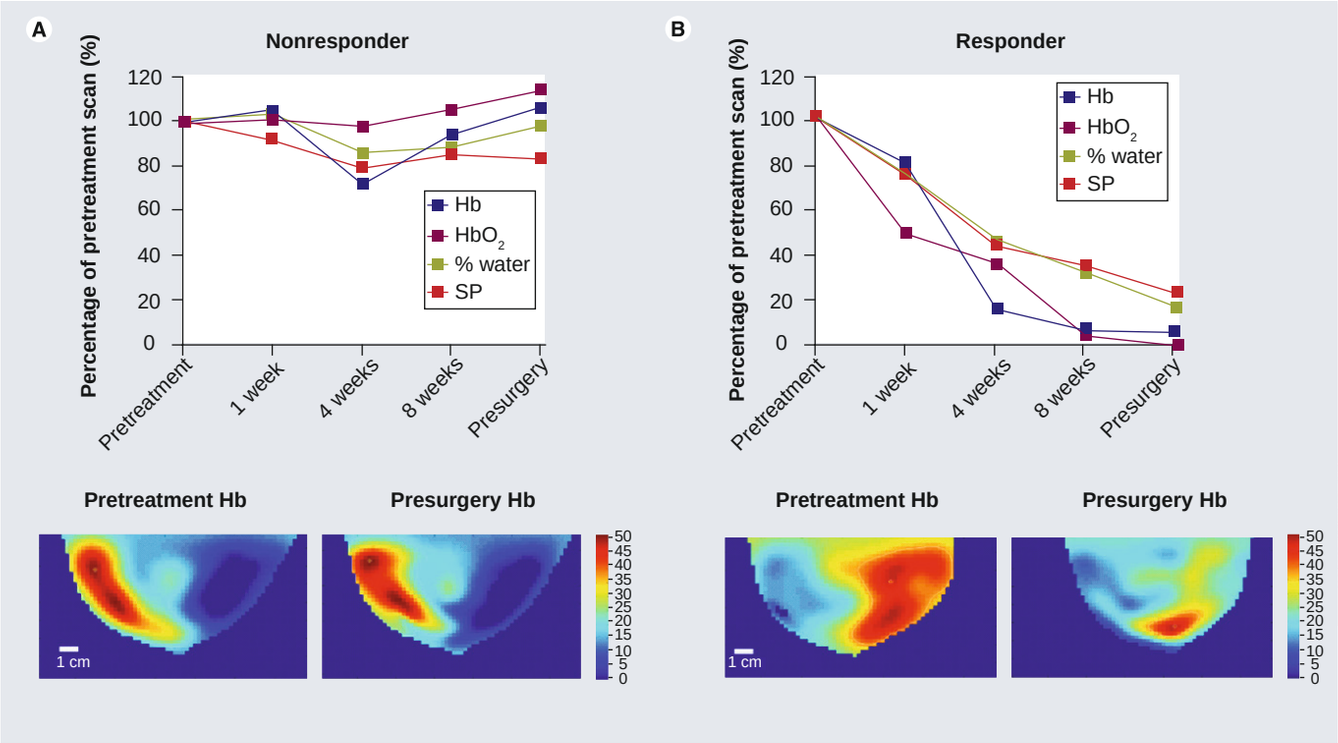

Figure 5. The application of diffuse optical imaging for evaluating cancer treatment response. Representative **(A)** nonresponders' versus **(B)** responders' data for Hb, HbO_2, water and SP. The graphs illustrate the percentage change from baseline in optical parameters during treatment. Also, shown are the corresponding pretreatment and presurgery diffuse optical imaging maps of Hb where 6% and -93% changes were obtained for the nonresponding and responding patients, respectively. Note that in the nonresponder there is a minimal change in the optical parameters from pretreatment to presurgery opposed to the responder, where a significant drop in all optical parameters is observed.
Hb: Dexyhemoglobin; HbO_2: Oxyhemoglobin; SP: Scattering power.
Reproduced with permission from Soliman *et al.* [125].

six orders of magnitude [128]. Therefore, typical photoacoustic images based on endogenous contrast depict either resolvable blood vessels, the aggregate signal from many nonresolvable blood vessels or combinations of both. Moreover, oxyhemoglobin and deoxyhemoglobin have different optical absorption spectra. Several groups have shown that by illuminating tissue successively with wavelengths that correspond to the hemoglobin and deoxyhemoglobin optical absorption spectral peaks, spatial maps of the total hemoglobin concentration and the oxygen saturation of hemoglobin can be generated [129–131]. A number of groups are now working on combining the oxyhemoglobin concentration measurements with volumetric blood flow to calculate the metabolic rate of oxygen [132]. These functional parameters are of great interest in the monitoring of treatment response. Finally, with the introduction of exogenous contrast agents, such as organic dyes or nanoparticles, specific structures can be targeted with high sensitivity. Examples include the use of intravenously injected indocyanine green (ICG) solutions to examine the function of kidneys [133], green fluorescent protein production [134,135] and gold nanoparticle distribution [136].

Since PAI is well suited for functional imaging based on the sensitivity to blood volume and oxygenation status, there is significant potential in the application of photoacoustics to cancer treatment monitoring. Work in the field of DOI (see 'DOI: evaluating tissue functional and structural changes' section) suggests that the absolute changes in the tumor/normal tissue ratio of deoxyhemoglobin concentration was the most sensitive indicator of pathological response to treatment [137]. Given the sensitivity of PAI to blood and its change in the absorption as a function of oxygenation status, it is expected to be more sensitive than the DOI counterpart and with better spatial localization. PAI is currently being explored in this capacity for combining such measurements with US imaging. The goal is to use QUS to monitor cell death, as explained in the 'QUS: monitoring cell death response' section, and PAI to probe blood volume, oxygenation status and estimate the metabolic rate of oxygen. There are significant advantages to this approach: US and photoacoustic images are naturally coregistered

and in both cases the endogenous contrast is used to assess the treatment response. US will be primarily used to probe cellular structure and function and photoacoustics will be primarily used to probe vascular structure and function, covering the two most important tissue elements of interest for cancer therapy monitoring: cancer cells and blood vessels.

Clinical PAI is still in its early stages and the main clinical target has been early tumor detection for breast cancer. Systems have been developed that use an array of 590 transducers to receive the photoacoustic signal and use a scanning stage so that the laser beam can be translated to illuminate the region of interest of the breast [138,139]. In pilot experiments, the investigators found that high-intensity regions in their 3D PAI datasets were associated with increased hemoglobin distributions that they attributed to vascularization characteristic to the malignancies examined. In another approach, a commercial US hand-held linear probe is used with side laser illumination that achieves and coregisters optoacoustic (functional) and US (anatomical) images [140]. The group has also reported unique signatures associated with malignancies, with regions of high vascularity in the tumor regions associated with strong photoacoustic signals. These early clinical results illustrate the potential of using these systems for imaging tumors and cancer treatment monitoring. Finally, several groups have reported on the changes that occur in the photoacoustic signals after thermal coagulation of tissues [141–143].

Future perspective

■ Radionuclide imaging

Radionuclide imaging methods are expanding as new molecules of clinical pertinence are discovered and as new probe agents are developed. It may be possible in the future to couple these relevant biomarkers for response detection and new probe designs for therapy purposes. The advantage of the technique is the specificity and sensitivity to cell death. However, the need to inject radionuclide at each time point for which an assessment of the tumor response is required, as well as the logistical and regulatory constraints of the administration of such radioactive agents, reduce the appropriateness of the technique for longitudinal studies of tumor response for which many imaging time points may be required.

■ MRI

Environment-sensitive methods of MRI have been demonstrated to be promising for detecting the cellular and microscopic-level changes of apoptosis. However, contrast agent methods for MRI can be limited in the ability to deliver contrast agent to the tissue of interest. For example, low contrast agent concentration makes parametric maps of exchange based on T_1 imprecise. Targeted contrast agents and contrast agents with higher relaxivities (stronger effect per unit concentration) would be of benefit in future work, as well as different injection strategies. Stronger magnetic fields are becoming more common in the clinic, including stronger gradients, which will benefit methods like oscillating gradient diffusion. In addition, different gradient waveforms may be examined that are capable of picking out ranges of frequencies or distance scales that are of interest in therapy response.

■ DCE-US

DCE-US is evolving alongside the developments of microbubble engineering and advancements in US imaging technology. Recently introduced 2D matrix arrays allow volumetric imaging of contrast agent perfusion in real time. Considered the new 'state of the art', 3D and 4D imaging overcomes some of the challenges of traditional US, which include: constrained spatial sampling to a single imaging plane at any one time; out of plane target motion that results in unrecoverable loss of data; and minimal control over the US beam width in the elevation direction [70]. 4D DCE-US can monitor microbubble kinetics in multiple imaging planes simultaneously, enabling a more rigorous interpretation of contrast kinetics flowing in and out of a volume of tissue and improving measurement reproducibility in heterogeneous tumors [144].

New applications of US imaging are emerging by virtue of developing US contrast agents. Submicron perflurocarbon droplets are currently being investigated as an extravascular contrast agent with capabilities to better detect small cancers and quantify vessel wall permeability [145]. Molecular imaging using US is made possible by engineering the encapsulating shell of the microbubble to contain ligands targeted to biological markers of disease [146–148]. Nevertheless, presently these markers remain limited to the vascular endothelium.

■ QUS

QUS methods can now be readily implemented using a number of commercially available high- and low-frequency US instruments. Coupled with information from carefully controlled biological experiments *in vitro* and *in vivo,*

investigators are arriving at well-formed understandings of structural features that influence QUS parameters. This has led to reproducible results in the differentiation of benign versus malignant disease and also for the detection of cell death. In a similar context, US strain and shear wave imaging, which can reflect tissue stiffness (as representatives of elastography), have also been hypothesized to have large contrast between treatment-responding and -nonresponding malignant tissues. These methods are currently available in a number of clinical US devices as well. Given the relatively low cost of US equipment, and the fact that contrast is generated by the process of cell death itself (i.e., without the need for the injection of contrast agents), it should be possible in the near future to start using these methods as

Executive summary

Background

- Imaging response to therapy has been of growing interest where various cellular and/or functional mechanisms are understood. Related development of therapies has benefited from the ability to monitor or predict responses to different treatments. Benefiting from different mechanisms as sources of imaging contrasts, a multimodality approach may provide a more informative tool for monitoring treatment response, compared with a single imaging modality or imaging mode.

Radionuclide imaging

- Radionuclide imaging has enabled cancer-associated contrast imaging in studies of cellular biology, biochemistry, metabolism and receptor expression. Owing to high specificity and sensitivity to cell death, these modalities can be used to detect treatment response by administering subpharmacological doses of agents. This avoids any adverse pharmacological effects from the labeled probe molecules. Recent studies have suggested the successful application of small-sized tracer molecules for fast tumor penetration and clearance.
- This modality, however, requires radionuclides and remains limited in resolution owing to limitations in emission detection. Moreover, the injection of radionuclides limits the number of times patients would be imaged during their therapy to assess tumor response.

MRI

- MRI methods sensitive to particular environments are presently promising for detecting the cellular and microscopic-level changes associated with cell death processes, such as apoptosis. These include the use of rotating frame relaxation and magnetization transfer to probe macromolecular changes and water influx; extracellular contrast agents that are sensitive to water exchange across the membrane, which can increase following the start of cell death; and diffusion with time-varying gradients, which is sensitive to changes at smaller distance scales than conventional diffusion and demonstrates an increase in the apparent diffusion for high gradient frequencies.
- Current methods of MRI, however, typically suffer from low signal-to-noise ratio, and consequently low sensitivity and specificity for the detection of cell death. Ongoing research attempts to address these issues by measuring more sensitive parameters associated with cell death.

Dynamic contrast-enhanced ultrasound

- Dynamic contrast-enhanced ultrasound inherits the strengths of diagnostic ultrasound imaging to be fast, portable, safe, widely available and cost effective. It leverages the unique properties of microbubble contrast agents to monitor therapeutics that rely upon and target blood perfusion.
- Unfortunately, due to regulatory hurdles, microbubble agents remain limited in their clinical approval in many countries.

Quantitative ultrasound

- Differentiable echogeneities exhibited by living and dead cells enables the monitoring of cell death response via quantitative ultrasound (QUS) techniques at high frequencies and recently at clinical range frequencies. In the near future, conventional frequency QUS is expected to provide rapid and quantitative functional information in real time, and at the patient bedside for evaluating therapy response early following treatment.
- Given the fact that ultrasound is not a volumetric modality and its 2D scan planes have a relatively limited field of view, finding the same nominal regions of interest throughout the different scan sessions during the course of treatment can be difficult. Although this usually is not the case for the first few weeks of treatment where the early prediction of treatment response is proposed to focus on, it would more likely be encountered afterwards especially when the tumor starts to shrink and alter. Employing 3D optical trackers during the scans to record physical coordinates of the scan planes, which enables 3D volume reconstruction, as well as acquiring several number of scan planes at each session to cancel out the sessions' variability, may address this issue to some extent.

Diffuse optical imaging

- Diffuse optical imaging is a noninvasive, nonionizing imaging modality that employs near-infrared light to provide tissue functional and structural information. Recent findings have demonstrated that this modality can be used to monitor treatment response in breast cancer patients.
- Owing to the high rates of attenuation of near-infrared light in soft tissues, the application of diffuse optical imaging is, however, primarily limited to breast and brain, presently.

Photoacoustic imaging

- Photoacoustic imaging (PAI) can be used to provide functional information about the response of the tumor vasculature to cancer treatments. PAI can be used in combination with QUS to better characterize tumor response in terms of changes in blood oxygenation as a function of treatment in combination with cell death.
- PAI is a relatively superficial modality, hence its early-stage clinical application is mainly limited to breast, presently.

noninvasive image-based biomarkers of tumor response to start personalizing cancer therapies.

■ DOI

DOI has been shown to be a favorable tomographic technique to provide information about tissue microstructure and its metabolic activities. In the last decade, this technique has emerged as a potential noninvasive and affordable imaging modality, particularly in breast cancer imaging. The information provided by this modality can be used in the future to customize treatment plans. Prior to treatment initiation, information provided by DOI can be used to predict the presence of hypoxia in the tumor, which will provide guidance on the proper treatment choice (hormone therapy vs hormone therapy plus radiation). In addition, owing to its nonionizing nature, DOI scans can be repeated frequently to provide useful information about tumor progression and response to treatment. This will allow the objective, rational change of ineffective therapies to effective ones at an early stage in treatment (within weeks), as opposed to many months later, which would lead to better outcomes and spare patients of unnecessary side effects.

■ PAI

Clinical PAI imaging is still in its infancy, but the introduction of commercial clinical systems is expected to have a significant impact in the near future. As the main source of endogenous contrast in PAI is blood, changes in blood volume and oxygenation status during cancer treatment, known to occur from studies in DOI are very promising parameters to be used as biomarkers of tumor response. Moreover, since US and photoacoustic images are naturally coregistered, QUS can be used to probe cellular structure and function while with the same instrument photoacoustics can be used to probe vascular structure and function. Finally, since the procedure does not use nonionizing radiation, the imaging can be repeated frequently to provide information about the response of cell death and the oxygenation state of the vasculature.

Acknowledgement

We thank A Giles for many years of dedicated assistance with experiments and technical support.

Financial & competing interests disclosure

O Falou holds a Canadian Breast Cancer Foundation – Ontario Region Postdoctoral Fellowship. MC Kolios holds a Tier 2 Canada Research Chair in Biomedical Applications of Ultrasound. GJ Czarnota holds a Cancer Care Ontario Research Chair in Experimental Therapeutics and Imaging. The research here was supported by the Terry Fox Foundation, Canadian Breast Cancer Foundation – Ontario Region, Canadian Institutes of Health Research and Natural Sciences and Engineering Council of Canada. Sunnybrook Health Sciences Centre holds patents on 'Detection of apoptosis using high-frequency ultrasound' and on 'Methods of monitoring cellular death using low frequency ultrasound'. The authors have no other relevant affiliations or financial involvement with any organization or entity with a financial interest in or financial conflict with the subject matter or materials discussed in the manuscript apart from those disclosed.

No writing assistance was utilized in the production of this manuscript.

References

Papers of special note have been highlighted as:
▪ of interest
▪▪ of considerable interest

1 Brindle K. New approaches for imaging tumour responses to treatment. *Nat. Rev. Cancer* 8(2), 94–107 (2008).

▪▪ **Comprehensive review of contemporary imaging methods for tumor response detection spanning clinically established imaging modalities in addition to newly-proposed methods still under development.**

2 Roberts C, Buckley DL, Parker GJM. Comparison of errors associated with single- and multi-bolus injection protocols in low-temporal-resolution dynamic contrast-enhanced tracer kinetic analysis. *Magn. Reson. Med.* 56(3), 611–619 (2006).

3 Banihashemi B, Vlad R, Debeljevic B, Giles A, Kolios MC, Czarnota GJ. Ultrasound imaging of apoptosis in tumour response: novel preclinical monitoring of photodynamic therapy effects. *Cancer Res.* 68, 8590–8596 (2008).

▪ **Presents the first *in vivo* use of quantitative high-frequency ultrasound to monitor tumour cell death response to anticancer treatments.**

4 American Cancer Society. *Cancer Facts and Figures 2007.* American Cancer Society, AL, USA (2007).

5 Mankoff DA, Mankoff DA, Dunnwald LK *et al.* Monitoring the response of patients with locally advanced breast carcinoma to neoadjuvant chemotherapy using [technetium 99m]–sestamibi scintimammography. *Cancer* 85(11), 2410–2423 (1999).

6 Giordano SH. Update on locally advanced breast cancer. *Oncologist* 8(6), 521–530 (2003).

7 Esteva FJ, Hortobagyi GN. Locally advanced breast cancer. *Hematol. Oncol. Clin. North Am.* 13(2), 457–472 (1999).

8 Hortobagyi G. Comprehensive management of locally advanced breast cancer. *Cancer* 66, 1387–1391 (1990).

9 De Lena M, Varini M, Zucali R *et al.* Multimodal treatment for locally advanced breast cancer. Result of chemotherapy–radiotherapy versus chemotherapy–surgery. *Cancer Clin. Trials* 4, 229–236 (1981).

10 Smith IC, Heys SD, Hutcheon AW *et al.* Neoadjuvant chemotherapy in breast cancer: significantly enhanced response with docetaxel. *J. Clin. Oncol.* 20, 1456–1466 (2002).

11 Chollet P, Charrier S, Brain E *et al.* Clinical and pathological response to primary chemotherapy in operable breast cancer. *Eur. J. Cancer* 33, 862–866 (1997).

12 Clarke M, Collins R, Darby S *et al.* Early Breast Cancer Trialists' Collaborative Group (EBCTCG). Effects of radiotherapy and of differences in the extent of surgery for early

breast cancer on local recurrence and 15-year survival: an overview of the randomised trials. *Lancet* 366(9503), 2087–2106 (2005).

13 Punglia RS, Morrow M, Winer EP, Harris JR. Local therapy and survival in breast cancer. *N. Engl. J. Med.* 356, 2399–2405 (2007).

14 Fisher B, Bryant J, Wolmark N *et al.* Effect of preoperative chemotherapy on the outcome of women with operable breast cancer. *J. Clin. Oncol.* 16(8), 2672–2685 (1998).

15 Yeh E, Slanetz P, Kopans DB *et al.* Prospective comparison of mammography, sonography, and MRI in patients undergoing neoadjuvant chemotherapy for palpable breast cancer. *Am. J. Roentgenol.* 184, 868–877 (2005).

16 Huang E, McNeese MD, Strom EA *et al.* Locoregional treatment outcomes for inoperable anthracycline-resistant breast cancer. *Int. J. Radiat. Oncol. Biol. Phys.* 53(5), 1225–1233 (2002).

17 Esteva FJ, Hortobagyi GN. Can early response assessment guide neoadjuvant chemotherapy in early-stage breast cancer? *J. Natl Cancer Inst.* 100(8), 521–523 (2008).

18 Gambhir SS. Molecular imaging of cancer with positron emission tomography. *Nature Rev. Cancer* 2, 683–693 (2002).

19 Smith TAD. The rate-limiting step for tumour [18F]fluoro-2-deoxy-D-glucose (FDG) incorporation. *Nucl. Med. Biol.* 28, 1–4 (2001).

20 Czernin J, Phelps ME. Positron emission tomography scanning: current and future applications. *Annu. Rev. Med.* 53, 89–112 (2002).

21 Schelling M, Avril N, Nährig J *et al.* Positron emission tomography using [18F] fluorodeoxyglucose for monitoring primary chemotherapy in breast cancer. *J. Clin. Oncol.* 18, 1689–1695 (2000).

22 Weber WA, Petersen V, Schmidt B *et al.* Positron emission tomography in non-small-cell lung cancer: Prediction of response to chemotherapy by quantitative assessment of glucose use. *J. Clin. Oncol.* 21, 2651–2657 (2003).

23 Spaepen K, Stroobants S, Dupont P *et al.* Prognostic value of positron emission tomography (PET) with fluorine-18 fluorodeoxyglucose ([^{18}F]FDG) after first-line chemotherapy in non-Hodgkin's lymphoma: is [^{18}F]FDG PET a valid alternative to conventional diagnostic methods? *J. Clin. Oncol.* 19, 414–419, (2001).

24 Shields AF, Mankoff DA, Link JM *et al.* Carbon-11-thymidine and FDG to measure therapy response. *J. Nucl. Med.* 39, 1757–1762 (1998).

25 van Waarde A, Been LB, Ishiwata K, Dierckx RA, Elsinga PH. Early response of sigma-receptor ligands and metabolic PET tracers to 3 forms of chemotherapy: an *in vitro* study in glioma cells. *J. Nucl. Med.* 47, 1538–1545 (2006).

26 Pio BS, Park CK, Pietras R *et al.* Usefulness of 3′-[^{18}F]fluoro-3′-deoxythymidine with positron emission tomography in predicting breast cancer response to therapy. *Mol. Imaging Biol.* 8, 36–42 (2006).

27 Ljungkvist ASE, Bussink J, Kaanders JHAM, van der Kogel AJ. Dynamics of tumour hypoxia measured with bioreductive hypoxic cell markers. *Radiat. Res.* 167, 127–145 (2007).

28 Eschmann SM, Paulsen F, Reimold M *et al.* Prognostic impact of hypoxia imaging with ^{18}F-misonidazole PET in nonsmall cell lung cancer and head and neck cancer before radiotherapy. *J. Nucl. Med.* 46, 253–260 (2005).

29 Gagel B, Reinartz P, Demirel C *et al.* [^{18}F] fluoromisonidazole and [^{18}F] fluorodeoxyglucose positron emission tomography in response evaluation after chemo-/radiotherapy of non-small-cell lung cancer: a feasibility study. *BMC Cancer* 6, 51 (2006).

30 Belhocine T, Steinmetz N, Hustinx R *et al.* Increased uptake of the apoptosisimaging agent 99mTc recombinant human Annexin V in human tumours after one course of chemotherapy as a predictor of tumour response and patient prognosis. *Clin. Cancer Res.* 8, 2766–2774 (2002).

31 Cauchon N, Langlois R, Rousseau JA *et al.* PET imaging of apoptosis with ^{64}Cu-labeled streptavidin following pretargeting of phosphatidylserine with biotinylated annexin-V. *Eur. J. Nucl. Med. Mol. Imaging* 34, 247–258 (2007).

32 Van Den Bossche B, De Wiele CV. Receptor imaging in oncology by means of nuclear medicine: current status. *J. Clin. Oncol.* 22, 3593–3607 (2004).

33 Linden HM, Stekhova VA, Link JM *et al.* Quantitative fluoroestradiol positron emission tomography imaging predicts response to endocrine treatment in breast cancer. *J. Clin. Oncol.* 24, 2793–2799 (2006).

34 Dehdashti F, Picus J, Michalski JM *et al.* Positron tomographic assessment of androgen receptors in prostatic carcinoma. *Eur. J. Nucl. Med. Mol. Imag.* 32, 344–350 (2005).

35 Orlova A, Magnusson M, Eriksson TL *et al.* Tumour imaging using a picomolar affinity HER2 binding affibody molecule. *Cancer Res.* 66(8), 4339–4348 (2006).

36 Orlova A, Wållberg H, Stone-Elander S, Tolmachev V. On the selection of a tracer for PET imaging of HER2-expressing tumours: direct comparison of a ^{124}I-labeled affibody molecule and trastuzumab in a murine xenograft model. *J. Nucl. Med.* 50(3), 417–425 (2009).

37 Tolmachev V, Orlova A, Nilsson FY, Feldwisch J, Wennborg A, Abrahmsén L. Affibody molecules: potential for *in vivo* imaging of molecular targets for cancer therapy. *Expert Opin. Biol. Ther.* 7(4), 555–568 (2007).

38 Chenevert TL, McKeever PE, Ross BD. Monitoring early response of experimental brain tumours to therapy using diffusion magnetic resonance imaging. *Clin. Cancer Res.* 3, 1457–1466 (1997).

39 Valonen PK, Lehtimäki KK, Väisänen TH *et al.* Water diffusion in a rat glioma during ganciclovir-thymidine kinase gene therapy-induced programmed cell death *in vivo*: correlation with cell density. *J. Magn. Reson. Imag.* 19(4), 389–396 (2004).

40 Sierra A, Michaeli S, Niskanen J-P *et al.* Water spin dynamics during apoptotic cell death in glioma gene therapy probed by T_1rho and T_2rho. *Magn. Reson. Med.* 59(6), 1311–1319 (2008).

41 Hakumäki JM, Gröhn OHJ, Tyynelä K, Valonen P, Ylä-Herttuala S, Kauppinen RA. Early gene therapy-induced apoptotic response in BT4C gliomas by magnetic resonance relaxation contrast T_1 in the rotating frame. *Cancer Gene Ther.* 9(4), 338–345 (2002).

42 Gröhn OHJ, Valonen PK, Lehtima KK, Va TH, Kauppinen RA, Garwood M. Novel magnetic resonance imaging contrasts for monitoring response to gene therapy in rat glioma. *Cancer Res.* 63, 7571–7574 (2003).

43 Bailey C, Desmond KL, Czarnota GJ, Stanisz GJ. Quantitative magnetization transfer studies of apoptotic cell death. *Magn. Reson. Med.* 66(1), 264–269 (2011).

44 Salhotra A, Lal B, Laterra J, Sun PZ, van Zijl PCM, Zhou J. Amide proton transfer imaging of 9L gliosarcoma and human glioblastoma xenografts. *NMR Biomed.* 21(5), 489–497 (2008).

45 Bailey C, Giles A, Czarnota GJ, Stanisz GJ. Detection of apoptotic cell death *in vitro* in the presence of Gd-DTPA-BMA. *Magn. Reson. Med.* 62(1), 46–55 (2009).

▪ **Detailed relaxation measurements of apoptotic cells *in vitro* at a range of extracellular contrast agent concentrations, modeled to account for the exchange of water across the cell membrane.**

46 Bell LK, Ainsworth NL, Lee S-H, Griffiths JR. MRI and MRS assessment of the role of the tumour microenvironment in response to therapy. *NMR Biomed.* 24(6), 612–635, (2011).

47 Zahra MA, Hollingsworth KG, Sala E, Lomas DJ, Tan LT. Dynamic contrast-enhanced MRI as a predictor of tumour response to radiotherapy. *Lancet Oncol.* 8(1), 63–74 (2007).

48 Donahue KM, Weisskoff RM, Chesler DA *et al.* Improving MR quantification of regional blood volume with intravascular T_1 contrast agents: accuracy, precision, and water exchange. *Magn. Reson. Med.* 36(6), 858–867 (1996).

49 Buckley DL, Kershaw LE, Stanisz GJ. Cellular-interstitial water exchange and its effect on the determination of contrast agent concentration *in vivo*: dynamic contrast-enhanced MRI of human internal obturator muscle. *Magn. Reson. Med.* 60(5), 1011–1019 (2008).

50 Landis CS, Li X, Telang FW *et al.* Equilibrium transcytolemmal water-exchange kinetics in skeletal muscle *in vivo*. *Magn. Reson. Med.* 42(3), 467–478 (1999).

51 Cheng HL. Investigation and optimization of parameter accuracy in dynamic contrast-enhanced MRI. *J. Magn. Reson. Imag.* 28(3), 736–743 (2008).

52 Kershaw LE, Cheng H-LM. A general dual-bolus approach for quantitative DCE-MRI. *Magn. Reson. Imaging* 29(2), 160–166 (2011).

53 Stanisz GJ. Diffusion MR in Biological systems: tissue compartments and exchange. *Israel J. Chem.* 43(1–2), 33–44 (2003).

54 Colvin DC, Jourquin J, Xu J, Does MD, Estrada L, Gore JC. Effects of intracellular organelles on the apparent diffusion coefficient of water molecules in cultured human embryonic kidney cells. *Magn. Reson. Med.* 65, 796–801 (2011).

55 Xu J, Does MD, Gore JC. Sensitivity of MR diffusion measurements to variations in intracellular structure: effects of nuclear size. *Magn. Reson. Med.* 61(4), 828–833 (2009).

56 Colvin DC, Loveless ME, Does MD, Yue Z, Yankeelov TE, Gore JC. Earlier detection of tumour treatment response using magnetic resonance diffusion imaging with oscillating gradients. *Magn. Reson. Imaging* 29(3), 315–323 (2011).

▪ **Uses an oscillating gradient diffusion sequence to monitor changes in a rat brain glioma model following chemotherapeutic treatment.**

57 Molls M, Vaupel P (Eds). *Blood Perfusion and Microenvironment of Human Tumours: Implications For Clinical Radiooncology.* Springer, NY, USA (1998).

58 Vaupel P. Tumour microenvironmental physiology and its implications for radiation oncology. *Semin. Radiat. Oncol.* 14(3), 198–206 (2004).

59 Hynynen K, Deyoung D, Kundrat M *et al.* The effect of blood perfusion rate on the temperature distributions induced by multiple, scanned and focused ultrasonic beams in dogs' kidneys *in vivo*. *Int. J. Hyperthermia* 5(4), 485–497 (1989).

60 Saleem A, Price PM. Early tumour drug pharmacokinetics is influenced by tumour perfusion but not plasma drug exposure. *Clin. Cancer Res.* 14(24), 8184–8190 (2008).

61 Yankeelov TE, Niermann Kenneth J, Huamani J *et al.* Correlation between estimates of tumour perfusion from microbubble contrast-enhanced sonography and dynamic contrast-enhanced magnetic resonance imaging. *J. Ultrasound Med.* 25 (4), 487–497 (2006).

62 Hudson JM, Leung K, Burns PN. The lognormal perfusion model for disruption replenishment measurements of blood flow: *in vivo* validation. *Ultrasound Med. Biol.* 37(10), 1571–1578 (2011).

63 Gorce JM, Arditi M, Schneider M. Influence of bubble size distribution on the echogenicity of ultrasound contrast agents: a study of SonoVueTM. *Invest. Radiol.* 35(11), 661–671 (2000).

64 Goertz DE, De Jong N, Van De Steen AFW. Attenuation and size distribution measurements of Definity™ and manipulated Definity™ populations. *Ultrasound Med. Biol.* 33(9), 1376–1388 (2007).

65 Lindner JR, Song J, Jayaweera AR *et al.* Microvascular rheology of definity microbubbles after intra-arterial and intravenous administration. *J. Am. Soc. Echocardiog.* 15(5), 396–403 (2002).

66 Eckersley RJ, Chin CT, Burns PN. Optimising phase and amplitude modulation schemes for imaging microbubble contrast agents at low acoustic power. *Ultrasound Med. Biol.* 31(2), 213–219 (2005).

67 Lampaskis M, Averkiou M. Investigation of the relationship of nonlinear backscattered ultrasound intensity with microbubble concentration at low MI. *Ultrasound Med. Biol.* 36(2), 306–312 (2010).

68 Lamuraglia M, Bridal SL, Santin M *et al.* Clinical relevance of contrast-enhanced ultrasound in monitoring anti-angiogenic therapy of cancer: current status and perspectives. *Crit. Rev. Oncol. Hematol.* 73(3), 202–212 (2010).

69 Lassau L, Chami L, Benatsou B *et al.* Dynamic contrast-enhanced ultrasonography (dce-us) with quantification of tumour perfusion: a new diagnostic tool to evaluate the early effects of antiangiogenic treatment. *Eur. Radiol. Suppl.* 17(Suppl. 6), 89–98 (2007).

70 Tang MX, Mulvana H, Gauthier T *et al.* Quantitative contrast-enhanced ultrasound imaging: a review of sources of variability. *Interface Focus* 1, 520–539 (2011).

▪▪ **Survey of functional ultrasound monitoring of cancer treatment using contrast agents.**

71 Wei K, Jayaweera A, Firoozan S *et al.* Quantification of myocardial blood flow with ultrasound-induced destruction of microbubbles administered as a constant venous infusion. *Circulation* 97(5), 473–483 (1998).

72 Arditi M, Frinking PJA, Rognin NG. A new formalism for the quantification of tissue perfusion by the destruction-replenishment method in contrast ultrasound imaging. *IEEE Trans. Ultrason. Ferroelectr. Freq. Control* 53(6), 1118–1129 (2006).

73 Hudson JM, Williams R, Lloyd B *et al.* Improved flow measurement using microbubble contrast agents and disruption-replenishment: clinical application to tumour monitoring. *Ultrasound Med. Biol.* 37(8), 1210–1221 (2011).

74 Meloni MF, Livraghi T, Filice C *et al.* Radiofrequency ablation of liver tumours: the role of microbubble ultrasound contrast agents. *Ultrasound Q.* 22(1), 41–47 (2006).

75 Slabaugh TK Jr, Machaidze Z, Hennigar R *et al.* Monitoring radiofrequency renal lesions in real time using contrast-enhanced ultrasonography: a porcine model. *J. Endourol.* 19(5), 579–583 (2005).

76 Kim CK, Choi D, Lim HK *et al.* Therapeutic response assessment of percutaneous radiofrequency ablation for hepatocellular carcinoma: utility of contrast-enhanced agent detection imaging. *Eur. J. Radiol.* 56(1), 66–73 (2005).

77 Krix M, Plathow C, Essig M *et al.* Monitoring of liver metastases after stereotactic radiotherapy using low-MI contrast-enhanced ultrasound initial results. *Eur. Radiol.* 15(4), 677–684 (2005).

78 Serra C, Menozzi G, Labate AMM *et al.* Ultrasound assessment of vascularization of the thickened terminal ileum wall in Crohn's disease patients using a low-mechanical index real-time scanning technique with a second generation ultrasound contrast agent. *Eur. J. Radiol.* 62(1), 114–121 (2007).

79 Bagi CM, Swanson T, Tuthill T. Use of ultrasound to assess drug efficacy in orthotopic rat models of HCC. In: *Ultrasound Imaging – Med. Applications. Minin, IV and Minin, OV.* InTech, Croatia, 283–294 (2011).

80 Lavisse S, Lejeune P, Rouffiac V *et al.* Early quantitative evaluation of a tumour vasculature disruptive agent AVE8062 using dynamic contrast-enhanced ultrasonography. *Invest. Radiol.* 43(2), 100–111 (2008).

81 Czarnota GJ, Kolios MC, Vaziri H *et al.* Ultrasonic biomicroscopy of viable, dead and apoptotic cells. *Ultrasound Med. Biol.* 23, 961–965 (1997).

82 Czarnota GJ, Kolios MC, Abraham J *et al.* Ultrasound imaging of apoptosis: high-resolution non-invasive monitoring of programmed cell death *in vitro*, *in situ* and *in vivo*. *Br. J. Cancer* 81(3), 520–527 (1999).

83 Taggart LR, Baddour RE, Giles A, Czarnota GJ, Kolios MC. Ultrasonic characterization of whole cells and isolated nuclei. *Ultrasound Med. Biol.* 33, 389–401 (2007).

84 Tunis AS, Czarnota GJ, Giles A, Sherar MD, Hunt JW, Kolios MC. Monitoring structural changes in cells with high frequency ultrasound signal statistics. *Ultrasound Med. Biol.* 31, 1041–1049 (2005).

85 Kolios MC, Czarnota GJ, Lee M, Hunt JW, Sherar MD. Ultrasonic spectral parameter characterization of apoptosis. *Ultrasound Med. Biol.* 28, 589–597 (2002).

86 Vlad RM, Alajez NM, Giles A, Kolios MC, Czarnota GJ. Quantitative ultrasound characterization of cancer radiotherapy effects *in vitro*. *Int. J. Radiat. Oncol. Biol. Phys.* 72, 1236–1243 (2008).

87 Brand S, Solanki B, Foster DB, Czarnota GJ, Kolios MC. Monitoring of cell death in epithelial cells using high frequency ultrasound spectroscopy. *Ultrasound Med. Biol.* 35, 482–493 (2009).

88 Vlad RM, Czarnota GJ, Giles A, Sherar MD, Hunt JW, Kolios MC. High-frequency ultrasound for monitoring changes in liver tissue during preservation. *Phys. Med. Biol.* 50, 197–213 (2005).

89 Vlad RM, Brand S, Giles A, Kolios MC, Czarnota GJ. Quantitative ultrasound characterization of responses to radiotherapy in cancer mouse models. *Clin. Cancer Res.* 15, 2067–2075 (2009).

90 Hughes MS, Marsh JN, Zhang H *et al.* Characterization of digital waveforms using thermodynamic analogs: detection of contrast-targeted tissue *in vivo*. *IEEE Trans. Ultrason. Ferroelectr. Freq. Control* 53, 1609–1616 (2006).

91 Wallace KD, Marsh JN, Baldwin SL *et al.* Sensitive ultrasonic delineation of steroid treatment in living dystrophic mice with energy-based and entropy-based radio frequency signal processing. *IEEE Trans. Ultrason. Ferroelectr. Freq. Control* 54, 2291–2299 (2007).

92 Guimond A, Teletin M, Garo E *et al.* Quantitative ultrasonic tissue characterization as a new tool for continuous monitoring of chronic liver remodelling in mice. *Liver Int.* 27, 854–864 (2007).

93 Yang M, Krueger TM, Miller JG, Holland MR. Characterization of anisotropic myocardial backscatter using spectral slope, intercept and midband fit parameters. *Ultrasonic Imag.* 29, 122–134 (2007).

94 Vered Z, Barzilai B, Mohr GA *et al.* Quantitative ultrasonic tissue characterization with real-time integrated backscatter imaging in normal human subjects and in patients with dilated cardiomyopathy. *Circulation* 76, 1067–1073 (1987).

95 Allison JW, Barr LL, Massoth RJ, Berg GP, Krasner BH, Garra BS. Understanding the process of quantitative ultrasonic tissue characterization. *Radiographics* 14, 1099–1108 (1994).

96 Takiuchi S, Rakugi H, Honda K *et al.* Quantitative ultrasonic tissue characterization can identify high-risk atherosclerotic alteration in human carotid arteries. *Circulation* 102, 766–770 (2000).

97 Kovacs A, Courtois MR, Weinheimer CJ *et al.* Ultrasonic tissue characterization of the mouse myocardium: successful *in vivo* cyclic variation measurements. *J. Am. Soc. Echocardiogr.* 17, 883–892 (2004).

98 Oelze ML, O'Brien WD Jr, Blue JP, Zachary JF. Differentiation and characterization of rat mammary fibroadenomas and 4t1 mouse carcinomas using quantitative ultrasound imaging. *IEEE Trans. Med. Imag.* 23, 764–771 (2004).

99 Mamou J, Oelze ML, O'Brien WD Jr, Zachary JF. Identifying ultrasonic scattering sites from three-dimensional impedance maps. *J. Acoust. Soc. Am.* 117, 413–423 (2005).

100 Czarnota GJ, Kolios MC. Ultrasound detection of cell death. *Imag. Med.* 2(1), 17–28 (2010).

▪▪ **Reviews newly developed methods as well as the required biological/physical backgrounds for cell death detection using quantitative ultrasound techniques.**

101 Kolios MC, Czarnota GJ. The potential use of ultrasound for the detection of cell changes in cancer treatment. *Future Oncol.* 5(10), 1527–1532 (2009).

102 Foster FS, Pavlin CJ, Harasiewicz KA, Christopher DA, Turnbull DH. Advances in ultrasound biomicroscopy. *Ultrasound Med. Biol.* 26(1), 1–27 (2000).

103 Papanicolau N, Azrif M, Ranieri S, Giles A, Czarnota GJ. Conventional-frequency detection of apoptosis *in vitro* and *in vivo*. *J. Ultrasound Med.* 27(S59), 411726 (2008).

104 Lee J, Banihashemi B, Papanicolau N *et al.* Novel low-frequency ultrasound detection of apoptosis *in vitro and in vivo*. Presented at: *American Association of Cancer Research Annual Meeting*, San Diego, CA, USA, 12–16 April 2008.

105 Papanicolau N. *Conventional Frequency Ultrasound Detection of Tumour Response In Vivo To Cancer Treatment Administration.* Ryerson University, ON, Canada (2009).

106 Papanicolau N, Dent R, Spayne J *et al.* Conventional frequency evaluation of tumour cell death response in locally advanced breast cancer patients to chemotherapy treatment administration. *J. Acoust. Soc. Am.* 128(4), 2365 (2010).

107 Cutler M. Transillumination as an aid in the diagnosis of breast lesions. *Surg. Gynecol. Obstetr.* 48, 721–729 (1929).

108 Ntziachristos V, Chance B. Probing physiology and molecular function using optical imaging: applications to breast cancer. *Breast Cancer Res.* 3(1), 41–46 (2001).

▪▪ **Comprehensive paper that addresses the capacity of optical imaging to detect and monitor treatment response in breast cancer.**

109 Tromberg BJ, Shah N, Lanning R *et al.* Non-invasive *in vivo* characterization of breast tumours using photon migration spectroscopy. *Neoplasia* 2(1–2), 26–40 (2000).

110 Leff DR, Warren OJ, Enfield LC *et al.* Diffuse optical imaging of the healthy and diseased breast: a systematic review. *Breast Cancer Res. Treat.* 108(1), 9–22 (2008).

111 Zhou C, Eucker SA, Durduran T *et al.* Diffuse optical monitoring of hemodynamic changes in piglet brain with closed head injury. *J. Biomed. Opt.* 14(3), 034015 (2009).

112 Joseph DK, Huppert TJ, Franceschini MA, Boas DA. Diffuse optical tomography system to image brain activation with improved spatial resolution and validation with functional magnetic resonance imaging. *Appl. Opt.* 45(31), 8142–8151 (2006).

113 Durduran T, Yu G, Burnett MG *et al.* Diffuse optical measurement of blood flow, blood oxygenation, and metabolism in a human brain during sensorimotor cortex activation. *Opt. Lett.* 29(15), 1766–1768 (2004).

114 Boas DA, Dale AM, Franceschini MY. Diffuse optical imaging of brain activation: approaches to optimizing image sensitivity, resolution, and accuracy. *Neuroimage* 23(Suppl. 1), S275–S288 (2004).

115 Siegel AM, Culver JP, Mandeville JB, Boas DA. Temporal comparison of functional brain imaging with diffuse optical tomography and fMRI during rat forepaw stimulation. *Phys. Med. Biol.* 48(10), 1391–1403 (2003).

116 Culver JP, Siegel AM, Stott JJ, Boas DA. Volumetric diffuse optical tomography of brain activity. *Opt. Lett.* 28(21), 2061–2063 (2003).

117 Culver JP, Durduran T, Cheung C, Furuya D, Greenberg JH, Yodh AG. Diffuse optical measurement of hemoglobin and cerebral blood flow in rat brain during hypercapnia, hypoxia and cardiac arrest. *Adv. Exp. Med. Biol.* 510, 293–297 (2003).

118 Shah N, Cerussi A, Eker C *et al.* Noninvasive functional optical spectroscopy of human breast tissue. *Proc. Natl Acad. Sci. USA* 98(8), 4420–4425 (2001).

119 Tromberg BJ, Cerussi A, Shah N *et al.* Imaging in breast cancer. diffuse optics in breast cancer: detecting tumours in pre-menopausal women and monitoring neoadjuvant chemotherapy. *Breast Cancer Res.* 7(6), 279–285 (2005).

120 Zonios G, Perelman LT, Backman V *et al.* Diffuse reflectance spectroscopy of human adenomatous colon polyps *in vivo*. *Appl. Opt.* 38(31), 6628–6637 (1999).

121 Cerussi A, Hsiang D, Shah N *et al.* Predicting response to breast cancer neoadjuvant chemotherapy using diffuse optical spectroscopy. *Proc. Natl Acad. Sci. USA* 104(10), 4014–4019 (2007).

122 Roblyer D, Ueda S, Cerussi A *et al.* Optical imaging of breast cancer oxyhemoglobin flare correlates with neoadjuvant chemotherapy response one day after starting treatment. *Proc. Natl Acad. Sci. USA*. 108(35), 14626–14631 (2011).

123 Choe R, Corlu A, Lee K *et al.* Diffuse optical tomography of breast cancer during neoadjuvant chemotherapy: a case study with comparison to MRI. *Med. Phys.* 32(4), 1128–1139 (2005).

124 Jakubowski DB, Cerussi AE, Bevilacqua F *et al.* Monitoring neoadjuvant chemotherapy in breast cancer using quantitative diffuse optical spectroscopy: a case study. *J. Biomed. Opt.* 9(1), 230–238 (2004).

125 Soliman H, Gunasekara A, Rycroft M *et al.* Functional imaging using diffuse optical spectroscopy of neoadjuvant chemotherapy response in women with locally advanced breast cancer. *Clin. Cancer Res.* 16(9), 2605–2614 (2010).

126 Zhou C, Choe R, Shah N *et al.* Diffuse optical monitoring of blood flow and oxygenation in human breast cancer during early stages of neoadjuvant chemotherapy. *J. Biomed. Opt.* 12(5), 051903 (2007).

127 Bell AG. Selenium and the photophone. *Nature* 22(569), 500–503 (1880).

128 Yao J, Wang LV. Photoacoustic tomography: fundamentals, advances and prospects. *Contrat Media Mol. Imag.* 6(5), 332–345 (2011).

▪▪ **Good overview of the current state of photoacoustic imaging.**

129 Wang X, Xie X, Ku G, Wang LV, Stoica G. Noninvasive imaging of hemoglobin concentration and oxygenation in the rat brain using high-resolution photoacoustic tomography. *J. Biomed. Optic* 11(2), 024015 (2006).

130 Stein EW, Maslov K, Wang LV. Noninvasive, *in vivo* imaging of blood-oxygenation dynamics within the mouse brain using photoacoustic microscopy. *J. Biomed. Opt.* 14(2), 020502 (2009).

131 Saha RK, Kolios MC. Effects of erythrocyte oxygenation on optoacoustic signals. *J. Biomed. Opt.* 16(11), 115003 (2011).

132 Yao J, Maslov KI, Zhang Y, Xia Y, Wang LV. Label-free oxygen-metabolic photoacoustic microscopy *in vivo*. *J. Biomed. Optic* 16(7), 076003 (2011).

133 Buehler A, Herzog E, Razansky D, Ntziachristos V. Video rate optoacoustic tomography of mouse kidney perfusion. *Optics Lett.* 35(14), 2475–2477 (2010).

134 Ntziachristos V, Razansky D. Molecular imaging by means of multispectral optoacoustic tomography (MSOT). *Chem. Rev.* 110(5), 2783–2794 (2010).

135 Wang LV. Multiscale photoacoustic microscopy and computed tomography. *Nat. Photonics* 3(9), 503–509 (2009).

136 Mallidi S, Joshi PP, Sokolov K, Emelianov S. On sensitivity of molecular specific photoacoustic imaging using plasmonic gold nanoparticles. *Conf. Proc. IEEE Eng. Med. Biol. Soc.* 6338–6340 (2009).

137 Cerussi AE, Tanamai VW, Hsiang D, Butler J, Mehta RS, Tromberg BJ. Diffuse optical spectroscopic imaging correlates with final pathological response in breast cancer neoadjuvant chemotherapy. *Philos. Transact. A Math Phys. Eng. Sci.* 369(1955), 4512–4530 (2011).

138 Piras D, Steenbergen W, van Leeuwen TG, Manohar SG. photoacoustic imaging of the breast using the twente photoacoustic mammoscope: present status and future perspectives. *IEEE J. Sel. Top. Quantum Electron.* 16(4), 730–739 (2010).

139 Manohar S, Kharine A, van Hespen JCG, Steenbergen W, van Leeuwen TG. The Twente Photoacoustic Mammoscope: system overview and performance. *Phys. Med. Biol.* 50(11), 2543–2557 (2005).

140 Zalev J, Kolios MC. Detecting abnormal vasculature from photoacoustic signals using wavelet-packet features. *Proc. SPIE* doi:10.1117/12.873911 (2011) (Epub ahead of print.

141 Cui H, Yang X. Real-time monitoring of high-intensity focused ultrasound ablations with photoacoustic technique: an *in vitro* study. *Med. Phys.* 38(10), 5345–5350 (2011).

142 Chitnis PV, Brecht H-P, Su R, Oraevsky AA. Feasibility of optoacoustic visualization of high-intensity focused ultrasound-induced thermal lesions in live tissue. *J. Biomed. Opt.* 15(2), 021313 (2010).

143 Soroushian B, Whelan WM, Kolios MC. Study of laser-induced thermoelastic deformation of native and coagulated *ex-vivo* bovine liver tissues for estimating their optical and thermomechanical properties. *J. Biomed. Optic* 15(6), 065002 (2010).

144 Elliott ST. Volume ultrasound: the next big thing? *Br. J. Radiol.* 81(961), 8–9 (2008).

145 Reznik N, Williams R, Burns PN. Investigation of vaporized submicron perfluorocarbon droplets as an ultrasound contrast agent. *Ultrasound Med. Biol.* 37(8), 1271–1279 (2011).

146 Villanueva FS, Wagner WR. Ultrasound molecular imaging of cardiovascular disease. *Nat. Clin. Cardiovasc. Med.* 5(Suppl. 2), S26–S32 (2008).

147 Lindner JR. Molecular imaging with contrast ultrasound and targeted microbubbles. *J. Nucl. Cardiol.* 11(2), 215–221 (2004).

148 Dayton P, Rychak J. Molecular ultrasound imaging using microbubble contrast agents. *Front. Biosci.* 12(23), 5124–5142 (2007).

■ Websites

201 Seno Medical Instruments. www.senomedical.com

202 VisualSonics, Inc. www.visualsonics.com

203 Endra Life Sciences. www.endrainc.com